Carbohydrate Polymers 98 (2013) 451–459

Contents lists available at SciVerse ScienceDirect

Carbohydrate Polymers

journal homepage: www.elsevier.com/locate/carbpol

Obtaining of new magnetic nanocomposites based on modified polysaccharide

Nita Tudorachi*, Aurica Chiriac

"Petru Poni" Institute of Macromolecular Chemistry, Gr. Ghica Voda Alley, 41A, 700487 Iasi, Romania

ARTICLE INFO

Article history:
Received 27 March 2013
Received in revised form 29 April 2013
Accepted 28 May 2013
Available online 4 June 2013

Keywords:
Carboxymethyl starch-g-polylactic acid
Magnetite
Nanocomposites

ABSTRACT

The study presents the preparation of some composite materials with magnetic properties by two different encapsulation methods of magnetite (Fe_3O_4) in a polymer matrix based on carboxymethyl starch-g-polylactic acid (CMS-g-PLA). The copolymer matrix used to obtain the magnetic nanocomposites was synthesized by grafting reaction of carboxymethyl starch (CMS) with D,L-lactic acid (DLLA), in the presence of Sn octanoate [$Sn(Oct)_2$] as catalyst. Magnetite was obtained by co-precipitation from aqueous salt solutions $FeCl_2/FeCl_3$ (molar ratio 1/2). The magnetic composites were prepared by precipitation method in acetone (non-solvent) of the DMSO solutions of magnetite and copolymer, and synthesis *in situ* of the nanocomposites. In the first case, the particle size measured by DLS-technique was 168 nm, and the magnetization was 46.82 emu/g, while after *in situ* synthesis, the composite materials showed smaller size (141 nm), but the magnetization was reduced (3.04 emu/g). The higher magnetization in the first case is due to the great degree of encapsulation of the magnetite, which was about 43.4 wt.%, compared to 4.37 wt.% for the *in situ* synthesis (determined by thermogravimetry). The CMS-g-PLA copolymer, magnetite, and the nanocomposites were characterized by infrared spectroscopy (FTIR), near infrared chemical imagistic (NIR-CI), dynamic light scattering (DLS) technique, X-ray diffraction (WAXD), scanning electron microscopy (SEM), vibrating sample magnetometer (VSM) and thermal analyses. Since the polymer matrix and magnetite are biodegradable and biocompatible, the magnetic nanocomposites can be used for conjugation of some drugs. The polymer matrix CMS-g-PLA acts as a shell, and vehicle for the active component, whereas magnetite is the component which makes targeting possible by external magnetic field manipulation.

1. Introduction

Synthetic polymers and natural macromolecules have been extensively studied as colloidal materials for nanoparticles production designed for drug delivery. Synthetic polymers have the advantage of high purity and reproducibility over natural polymers. Among the synthetic polymers, the polyesters family *i.e.*, poly(lactic acid) (PLA), poly(ε-caprolactone) (PCL), poly(glycolic acid) (PGA), poly(lactide-co-glycolide) (PLGA), poly(β-hydroxybutyrate) (PHB), poly(3-hydroxybutyrate-*co*-3-hydroxyvalerate) (PHBV), poly(*p*-dioxanone) (PPDO), or other families such as poly(cyanoacrylates), poly(acrylic acid) (PAA), poly(anhydrides), poly(amides) (PA), poly(ortho esters) (PES), poly(ethylene glycol) (PEG), and poly(vinyl alcohol) (PVA) are suitable for drug delivery due to their biodegradability, special release profiles and biocompatibility (Barratt, 2000; Ghosh, 2004). In particular, PLGA has been Food and Drug Administration (FDA) approved for human therapy (Anderson & Shive, 1997). The magnetic polymeric nanoparticles (MPNPs) made from organic and inorganic components have unique characteristics due to the specific properties of the composites. The constituents of a MPNP play different roles: the polymeric matrix acts as a shell, reservoir, and vehicle for the active component, whereas magnetite is the component which makes targeting possible by external magnetic field manipulation. Functionalized biodegradable magnetic nanospheres and microspheres can be used for delivery of active components such as drugs (Barrat et al., 2000; Brigger, Dubernet, & Couvreur, 2002; Hans & Lowman, 2002; Wang, Xing, Li, Fu, & Li, 2012), vaccines (Al-Deena, Selomulya, & Williams, 2013; Kreuter, 1994), proteins (Blanco & Alonso, 1997), DNA (Oster et al., 2004; Panyam & Labhasetwar, 2003), enzymes (Kouassi, Irudayaraj, & McCarty, 2005; Sui et al., 2012). Also, biosensor development (Nakache, Poulain, Candau, Orecchioni, & Irache, 2000), imaging (Chung et al., 2012; Tartaj, Morales, Veintemillas-Verdaguer, Gonzalez-Carreno, & Serna, 2003), bioseparation (Bucak, Jones, Laibinis, & Hatton, 2003), hyperthermia (Baba et al., 2012; Pankhurst, Connolly, Jones, & Dobson 2003), targeted diagnostics and therapy (Levy, Sahoo, Kim, Bergey, & Prasad, 2002) are some of the many biomedical areas where magnetic

* Corresponding author. Tel.: +40 0766 316517; fax: +40 232 211299.
E-mail address: tudorachinita@yahoo.com (N. Tudorachi).

0144-8617/$ – see front matter © 2013 Elsevier Ltd. All rights reserved.
http://dx.doi.org/10.1016/j.carbpol.2013.05.080

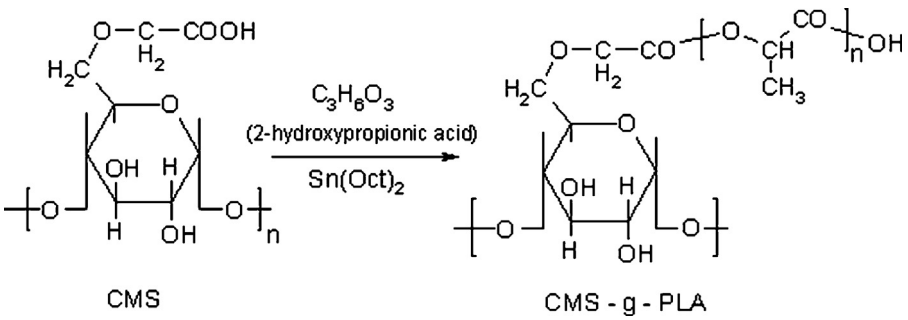

Scheme 1. The possible reaction of CMS-g-PLA copolymer synthesis.

nanoparticles could be of relevant use. Generally, the size and size distribution of the magnetic polymeric nanoparticles among other physical characteristics are affected by the technique used for the nanoparticle production and the pertinent synthesis parameters, *i.e.* molecular weight of the polymers, the addition of active components, surfactants, and other additives (Barrat et al., 2000; Brigger, Dubernet, & Couvreur, 2002; Chorny, Fishbein, Danenberg, & Golomb, 2002; Rao, Satish Kumar, Mathivanan, & Bhanoji Rao, 2003). Methods available for the nanoparticle synthesis can be divided into two classes: the first class comprises techniques such as emulsion or microemulsion polymerization, polycondensation, polymerization (radicalic, cationic, anionic), interfacial polymerization, and precipitation polymerization employ a monomer as a starting point, to form a magnetic core with a polymer shell. The second class includes emulsion evaporation, emulsion diffusion, solvent displacement, the miniemulsion technique and salting out when the nanoparticles are prepared from the already preformed polymer. In the last case, the starting materials are the polymer and magnetite, and no chemical reaction is involved in the process; the magnetite is entrapped into the polymeric matrix by hydrophobic–hydrophilic, electrostatic, or steric interaction. Lee et al. (2004) entrapped magnetite in PLGA by nanoprecipitation. The magnetite was suspended in acetone after the PLGA dissolution, and the initial magnetite concentration (theoretical loading) was 3.33% (w/w) (related to PLGA weight). The size of the obtained nanoparticle ranged from 120 nm to 230 nm for PLGA concentration varied from 1% to 5%, respectively. The emulsion evaporation method has been extensively used to entrapment of drugs (Hara et al., 2006; Song et al., 1997; Yan et al., 2002). The versatility of emulsion evaporation method permits to entrap magnetite by double emulsion process due to the hydrophilic behavior of magnetite, although hydrophilic compounds (normal magnetite) can be tailored to hydrophobic compounds by addition of a surfactant layer (oleic acid) to the particle surface. This magnetite surface modification ensures its entrapment in the PLGA (hydrophobic polymer) matrix by emulsion evaporation method.

The study presents the synthesis and characterization of some magnetic nanocomposites based on modified polysaccharide. The polymer matrix was carboxymethyl starch-g-poly(lactic acid) obtained by grafting reaction of carboxymethyl starch with D,L-lactic acid, and magnetite was obtained by co-precipitation technique from aqueous salt solutions Fe (II) and Fe (III) in alkaline medium.

2. Materials and methods

2.1. Materials

Carboxymethyl starch was synthesized in the laboratory by reacting corn starch with monochloroacetic acid, according to our previous paper (Tudorachi & Chiriac, 2008). The monomer D,L-lactic acid, (aqueous solution 90 wt.%, 1.21 g cm^{-3} density), dimethylsulfoxide (DMSO), tin (II) 2-ethylhexanoate (95 wt.% purity, 1.25 g cm^{-3} density), sodium hydroxide (Sigma Aldrich Chemie) were analytical grade reagents, and used without further purification. Magnetite was obtained in laboratory, by co-precipitation from aqueous salt solutions $FeCl_2/FeCl_3$ (molar ratio 1/2), by the addition of a base (pH = 10–12), under inert atmosphere (N_2), at 60 °C temperature, according to some methods described in the literature (Lu, Salabas, & Schuth, 2007), with particle size of about 249 nm. Poly(ethylene oxide)–poly(propylene oxide)–poly(ethylene oxide) non-ionic amphiphilic block copolymer (Pluronic F 127), as stabilizing agent for Fe_3O_4 nanoparticles, has been used. Acetone, isopropanol, methanol, acetic acid from Chimopar S.A. (Romania), were analytical reagents.

2.2. Synthesis of CMS-g-PLA copolymer

The carboxymethyl starch-g-polylactic acid copolymer was obtained by grafting reaction of carboxymethyl starch (CMS) with D,L-lactic acid, in the presence of $Sn(Oct)_2$, as catalyst. CMS was synthesized in laboratory by reacting of starch with monochloroacetic acid in strong alkaline medium (NaOH 40%) by dispersion in isopropyl alcohol, according to some slightly modified methods presented in the literature (Jiang et al., 2011; Stojanovič, Jeremič, & Jovanovič, 2000; Stojanovič, Jeremič, Jovanovič, & Lechnerb, 2005). CMS obtained and further used in synthesis of the CMS-g-PLA copolymer had the degree of substitution of about DS = 0.42, as determined by titration with 0.05 M HCl (Assaad, Wang, Zhu, & Mateescu, 2011). CMS-g-PLA synthesis was done in reaction vessel (250 ml) equipped with mechanical stirrer, thermostated oil bath, Dean–Stark distillation apparatus, vacuum valve, and dosing funnel reactants. The molar ratio of the CMS/D,L-lactic acid was 1/30, and $Sn(Oct)_2$ introduced in system was 0.9%, related to the two reactants. Approximately 0.009 mol (2 g) CMS were dissolved in 30 ml distilled water, under stirring at a temperature of 80 °C for 3 h. Next, the temperature was raised to 95–100 °C and under vacuum were easily removed about 15 ml of water used to dissolve CMS, by distillation trap. Then, the temperature decreased to 50 °C and under continuous stirring were added by the dripping funnel 0.27 mol (24 g) D,L-lactic acid (90% aqueous solution). After complete homogenization of the reactants were added dropwise 0.2 ml $Sn(Oct)_2$, alcoholic solution (d = 1.251 g cm^{-3}). Grafting reaction by polycondensation was carried out under vacuum at 110 °C, for 8 h, and at 120–125 °C for 7 h. Total volume of the products (water used as solvent and that resulting from the polycondensation reaction, the lactic acid unreacted and its oligomers) removed from the system was 35 ml. The resulting product shows high viscosity at high temperature and hardens by cooling. CMS-g-PLA copolymer was dried under vacuum at 65–70 °C, for 48 h. The CMS-g-PLA copolymer shows solubility in organic solvents

such as: DMSO, DMF, and toluene. The molecular weight of CMS-g-PLA copolymer (solvent DMSO) determined by DLS technique, was 38.29 kDa. Scheme 1 illustrates the proposed reaction mechanism.

2.3. Preparation of magnetic nanocomposites CMS-g-PLA/magnetite

To obtain composite materials with magnetic properties two methods have used: the precipitation method of magnetite and CMS-g-PLA copolymer solutions in a non-solvent (variant I), and *in situ* preparation of the composite material by introducing magnetite in the reaction mass for the CMS-g-PLA synthesis (variant II).

Variant I: The CMS-g-PLA copolymer synthesized in laboratory was dissolved in DMSO, at room temperature yielding a clear solution of 20 wt.% concentration. Subsequently, 10 g copolymer solution has been dispersed using an ultrasounds bath, for 3 min. In parallel, 0.8 g magnetite was dispersed with the ultrasounds bath for 3 min also in DMSO. Theoretical percentage of magnetite relative to copolymer matrix was 40 wt.%. At the magnetite suspension located in the ultrasounds bath, has been added the copolymer solution by dropwise and the ultrasonic operation continued for another 3 min. After homogenization, the suspension thus obtained was poured dropwise into a volume of 25 ml acetone also located in the ultrasounds bath. Acetone being a non-solvent, determines the precipitation of the copolymer on the surface of the magnetic nanoparticles, and obtaining the magnetic particles type core-shell coated with copolymer layer.

Variant II: The molar ratio of reactants and working conditions for *in situ* preparation of the magnetic nanocomposite CMS-g-PLA/magnetite were similar to those for the synthesis of the CMS-g-PLA copolymer. Approximately 2 g CMS were dissolved in 20 ml distilled water in the reaction vessel, at which it was added under stirring an aqueous suspension of magnetite (20 ml, concentration 5 wt.%) which was previously dispersed by ultrasonic operation in 24 g of D,L-lactic acid (90 wt.% aqueous solution). Theoretical percentage of magnetite relative to copolymer was 4.24 wt.%. After mixing for 30 min at a temperature of 40–50 °C, it was added $Sn(Oct)_2$ as catalyst (0.9 wt.% reported to reactants) and the reaction continued in the same temperature regime, as in the case of copolymer synthesis. The product obtained shows high viscosity, homogeneous and uniform distribution of the magnetite nanoparticles. The obtained magnetic nanoparticles were precipitated in acetone and dried under vacuum at 50–60 °C, for 48 h.

2.4. Fourier transform infrared (FTIR-ATR)

The spectra were recorded on a Vertex 70 spectrophotometer with ATR (Bruker-Germany). The vibrational transition frequencies were reported in wavenumbers (cm^{-1}) and the FTIR spectra were recorded on 600–4000 cm^{-1} interval, with a resolution of 4 cm^{-1}.

2.5. Near infrared chemical imagistic (NIR-CI)

This technique combines near infrared spectroscopy with high resolution imaging, in order to obtain the concentration of the compounds in composite, by visualizing the spatial distribution of the chemical compounds in a sample, provided by a chemical image. The measurements were recorded using a Specim's Ltd. SisuCHEMA apparatus and processed by "Evince" software. The system includes a Chemical Imaging Workstation for 1000–2500 nm NIR domains. The original image for each sample was taken with a NIR model spectral camera, respectively an imaging spectrograph type ImSpector N17E with 640 pixels spatial resolution at a rate of 60–350 Hz. The measurements implies the generation of the hyperspectral data cubes, containing thousands of spectra, which are afterwards processed by NIR-CI analysis, using "Evince" software. Partial least squared discriminate analysis model (PLS-DA) involves the building of the mathematical model using a lot of data to quantify the unknown component value based on the initial components. The final images have a complete spectrum that includes contributions from all the chemical components present in the sample. The calibration of the device was made using the NIR data of the initial components.

2.6. Thermogravimetric analyses (TG-DTG)

TG analyses were performed by means of a STA 449F1 Jupiter thermobalance (Netzsch-Germany). Samples with a mass ranging from 7 to 10 mg were heated from 30 to 620 °C in open Al_2O_3 crucible, with a heating rate of 10 °C min^{-1}. Nitrogen gas (99.99% purity), as carrier with flow rate of 50 mL min^{-1} and Al_2O_3 crucible (as reference material), were used.

2.7. The particle size distribution and average molecular weight

Size distribution and molecular weight were determined by dynamic light scattering (DLS) technique using a Zetasizer Nano-ZS device, ZEN-3500 model (Malvern Instruments-England). The hydrodynamic diameter and polydispersity were determined using noninvasive backscatter (NIBS) technology, which allows sample measurement in the range of 0.6 nm–6 μm. For measurement, the samples were dispersed in dispersant medium (twice distilled water, acetone) at a concentration of 1 g/L for size analysis and in DMSO at a concentration between 0.02 and 0.08 wt.% for the molecular weight. The measurement was carried out using a laser green light He–Ne (532 nm) as light source at a fixed angle of 173°. For each determination were made five measurements at 25 °C temperature.

2.8. Scanning electron microscopy (SEM)

The morphology Fe_3O_4 nanoparticles was studied using a SEM/ESEM-Edax-Quanta 200 apparatus, equipped with a large field detector. The acceleration voltage was 20 kV, under low vacuum mode 60–100 Pa.

2.9. Wide angle X-ray diffraction (WAXD)

The Fe_3O_4 nanoparticles were characterized using a Bruker AXS D8 Advance diffractometer, with scintillation detector in Bragg–Bretagne geometry, copper anode, X-ray tube type Siemens KFL-Cu 2 K, at $U = 36$ kV and 30 mA emission current.

2.10. Vibrating sample magnetometer (VSM)

The magnetite and CMS-g-PLA/magnetite composites (variants I and II) were analyzed with Lakeshore VSM 7400 system, to measure the magnetization at 25 °C. To avoid vibration of the particles, the samples were mixed with molten bees wax, cooled, to form a spherical solid sample of 8 mm.

3. Results and discussions

3.1. Characterization of CMS-g-PLA copolymer

3.1.1. FTIR and NIR spectroscopy

FTIR-ATR spectra of CMS and CMS-g-PLA copolymer are given in Fig. 1. In the FTIR spectrum of CMS is noted the presence of the characteristic absorption bands of starch, and other additional bands which appeared by modifying starch with monochloroacetic

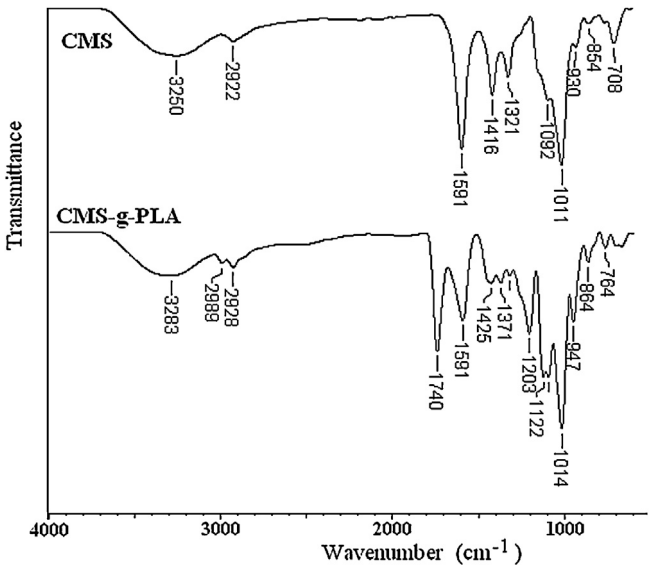

Fig. 1. FTIR-ATR spectra of CMS and CMS-g-PLA copolymer.

acid, data which are in agreement with the literature (Jiang et al., 2011; Lawal, Lechner, & Kulicke 2008). Some of these absorption bands are found and in the FTIR spectrum of the grafted copolymer. Thus, it can be seen a peak wider at 3250 cm^{-1} due to stretching vibrations of OH groups and other at 2922 cm^{-1} assigned to νCH_2 stretching vibrations. The peaks at 1591, 1416 and 1321 cm^{-1} were assigned to νCO asymmetric groups and νCOO^- symmetric groups of carboxyl group; bands at 1011 and 1092 cm^{-1} represent the aliphatic ether groups C—O—C existing in CMS. Bands at 708 and 854 cm^{-1} are caused by stretching vibrations of glycosidic structure of starch. In FTIR spectrum of the synthesized copolymer are observed characteristic absorption bands of structural units of PLA, as well as those belonging to CMS structure. One of the most important bands is at 1740 cm^{-1} which belongs $\nu C{=}O$ stretching vibrations of ester group, confirming that the esterification reaction occurred. Other absorption bands can be observed in the FTIR spectrum of the copolymer at 2989 and 2928 cm^{-1} characteristic to νCH_3 aliphatic groups and νCH respectively, of PLA grafted on CMS. Asymmetric and symmetric deformation vibrations $\delta asCH_3$ and δsCH_3 were recorded at 1425 and 1371 cm^{-1} respectively, for PLA grafted. The band at 1270 cm^{-1} is attributed to νCH_2 group, and bands present between 1014 and 1122 cm^{-1} are assigned to aliphatic ether groups (C—O—C), existing in CMS grafted.

The chemical structure of CMS-g-PLA copolymer was also confirmed by NIR spectroscopy. This technique allows monitoring the functional groups belonging to the CMS and PLA components. The signals for each functional group are assigned using IR reference spectra, available in the NIST libraries (http://webbook.nist.gov/chemistry/name-ser.html). Table 1 presents the NIR main absorption bands, on the 1100–2500 nm domain, extracted from NIR spectra belonging to CMS-g-PLA copolymer and comparatively to the CMS, PLA components. The CMS-g-PLA spectrum shows some specific bands belonging to both CMS and PLA components. The CH stretching first and second overtone corresponding to aliphatic groups in CMS, PLA and CMS-g-PLA structures, the OH stretching first overtone in ROH groups, the CO stretching second overtone in ester or acid groups of the components, OH combination bands were observed in all spectra and their intensities are relatively similar.

NIR-CI was also used to provide qualitative and quantitative analysis of the chemical composition. NIR-CI technique makes the fusion between near infrared spectroscopy and image analysis, in order to obtain the concentration of the compounds, by visualize the spatial distribution of the chemical compounds in a sample, provided by a chemical image. The sample measurement implies the generation of the hyperspectral data cubes containing thousands of spectra, which are after processed through NIR-CI analysis. The obtained spectra was decomposed into a set of small number of the classification scores using PLS-DA analysis model, where the score PLS-DA was obtained by correlating the information between the spectral data and the components ratio. The micrographs presented in Fig. 2 shows the score images obtained from each component and copolymer. The white and dark colors are attributed to the components, and the gray color is specific to the copolymer. The predominant gray color in copolymer highlights the uniform dispersion of PLA in the CMS-g-PLA structure. The average content of CMS and PLA in copolymer based on the images score is 26.4% (CMS) and 73.6% (PLA), a satisfactory result considering the molar ratio between components used in synthesis. NIR technique is generally more accurate for blends with physical bonds between components.

The nanoparticle size of CMS-g-PLA copolymer measured by DLS technique (acetone as solvent) was of 374 nm, and polydispersity index 0.297.

3.1.2. Characterization of magnetic nanoparticles

The magnetite used for the composite preparation is uniform with spherical or ellipsoidal form, without agglomeration as it is illustrated by SEM image (Fig. 3a). Pluronic F127 was used to stabilize the Fe_3O_4 nanoparticles. This stabilizer was reported as being one of the most effective in terms of stabilization, due to the hydrophilic chain length of poly(ethylene oxide) (Rahme, Gauffre, Marty, Payre, & Mingotaud, 2007). The saturation magnetization of 62.78 emu/g was determined from the VSM curve plateau (Fig. 3b), and remanent magnetization was of about 3.02 emu/g. At room temperature, in zero magnetic field the magnetic remanence was zero and the feature loop was anhysteretic, indicating that the magnetic nanoparticles are superparamagnetic. The magnetic composites must have sufficient magnetic properties and superparamagnetism for use in the medical field. To confirm the presence crystalline of naked Fe_3O_4 nanoparticles, the structure was characterized by WAXD and the diffractogram is shown in Fig. 3c. There are six main diffraction peaks for naked Fe_3O_4, which is the standard curve pattern for crystalline magnetite with spinel structure and were not observed characteristic peaks of other impurities.

Table 1
NIR signals for CMS-g-PLA copolymer, CMS and PLA.

NIR absorption bands	Wavenumber (nm)		
	CMS-g-PLA	CMS	PLA
—CH stretching second overtone in CH, CH_2, CH_3 groups	1180, 1200	1200	1180
—OH stretching first overtone in ROH group	1450	1450	1450
—CH stretching first overtone in CH, CH_2, CH_3 groups	1680, 1700	1780, 1800	1680, 1700
—C=O stretching first overtone in acid groups RCOOH, and ester groups RCOOR'	1820, 1950	1950	1950
—OH combination bands	2100	2100	2100
—CH symmetric stretch and bending combinations in CH, CH_2, CH_3 groups	2250	2310	2250–2400

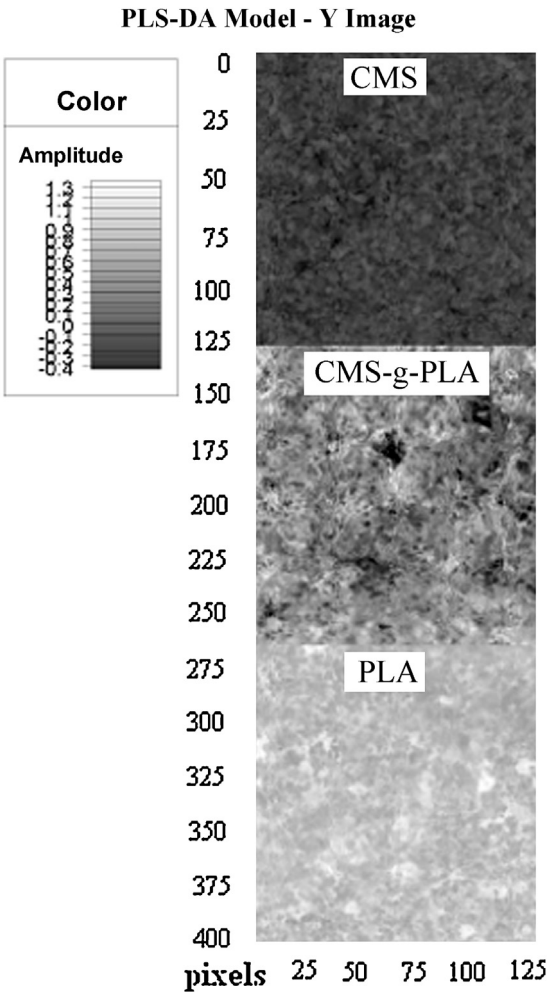

Fig. 2. The score images of CMS, PLA and CMS-g-PLA derived from PLS-DA.

Data are in good agreement with the literature values for magnetite (Fjellvag, Gronvold, Stolen, & Hauback, 1996; Ma, Guan, & Liu, 2005). The particles size of about 249 nm with PDI 0.260 and sizes distribution are presented in Fig. 3d. The saturation magnetization higher, but especially the remanence magnetization can boost attraction and agglomeration between magnetite particles leading to a slight increase in time of their size.

3.2. Characterization of CMS-g-PLA/magnetite composites

3.2.1. FTIR spectroscopy

FTIR spectra of CMS-g-PLA composites made by the two preparation variants are shown in Fig. 4. Firstly, the magnetite spectrum shows the peak of 573 cm^{-1}, which is attributed to the Fe—O bond vibration of Fe_3O_4 (Cornell & Schwertmann, 1996; Ma et al., 2003). Appearance of the peaks at 2941, 2893, 2889, 1612 and 1398 cm^{-1} shows that binding of Pluronic F 127 with Fe_3O_4 was occurred. These peaks are characteristic of asymmetric groups νCH_2, δCH_2 groups and C—O—C groups from poly(ethylene oxide)–poly(propylene oxide)–poly(ethylene oxide) bloc copolymer used to stabilize the magnetic nanoparticles. The hydroxide groups at surface (O—H stretching vibrations) of Fe_3O_4 nanoparticles are present at 3435 cm^{-1}. These groups can react further with the carboxylic groups from CMS-g-PLA and form the iron carboxylate COOM (M = metal ion) and hydrogen bonding, giving better stability to magnetite/copolymer composite (Xu, Shen, Xu, & Li, 2004). The intensity and width of this peak more pronounced in the magnetic composites (var. I and II), confirms the formation of the hydrogen bonds and metallic carboxylate groups. The magnetic composites FTIR spectra present absorption bands which found as well in the magnetite spectrum or that of CMS-g-PLA copolymer (shown in Fig. 1). The presence of these IR absorption bands confirms the organic/inorganic structure of the prepared magnetic composites.

3.2.2. Size distribution

The coated particle surface of magnetite consists of functionalized copolymer, which aims to subsequent coupling of drugs, can influence the particle size of magnetic composites. Thus, the nanoparticle size was 168 nm, with polydispersity index of 0.171 in the case of magnetic composite prepared through variant I, respectively 141 nm and polydispersity index 0.471 in the case of magnetic composite done with variant II (Fig. 5). The decrease of the magnetic composites particle size compared with those of pure magnetite (249 nm), is justified by the coverage with the compatible polymeric matrix – which may functioning as dispersing agent as well – on the surface of magnetic nanoparticles. The new shell is hindering the magnetic dipolar attraction between magnetic nanoparticles and favors the dispersion of magnetic nanoparticles in liquid media. This aspect is sustained by the saturation magnetization decrease at 46.82 emu/g (variant I) and 3.04 emu/g (variant II), and remanent magnetization of 2.2 emu/g (variant I) and 0.32 emu/g (variant II) due to the polymer layer. As it is well known when a compound is adsorbed on a surface, it generally does not lie flat. Rather, some parts of the polymer are adsorbed on the surface, while other portions of the chains extend away from the surface into the medium. Smaller dimensions for the magnetic composite resulted from *in situ* process are attributed to the initial complexation between magnetite surface and carboxyl groups of the lactic acid, followed by the grafting reaction. After that, the achievement of the core/shell magnetic composite is made with the smallest dimension of the particles assured by the macromolecular chains conformation which ensures as well the maximum stability for the system. In case of the first variant of preparation *CMS-g-PLA* adsorption on the magnetite surface takes place with the already realized conformation and steric hindrances of the copolymer. Moreover nor the synthesis conditions – time and temperature – were not the same. Both aspects can justify higher dimension registered for the magnetic composite achieved with the first variant of preparation.

Thus prepared magnetic composites have size of the nanometers order, which recommend their use in medical applications for the controlled and targeted delivery systems of the bioactive compounds.

3.2.3. Magnetization

The magnetic properties of composites CMS-g-PLA/magnetite (variants I and II of preparation) are shown in Fig. 6. The curves aspect indicates the prepared composites are superparamagnetic; this is attributed to the fact that the magnetic nanoparticles included in the polymer matrix were so small that they may be considered to have a single magnetic domain, phenomenon observed by other authors, too (Xuan et al., 2007). The saturation magnetization (var. I) is 46.82 emu/g, the remanent magnetization 2.2 emu/g under applied magnetic field of 24 Oe, indicating that the superparamagnetism of magnetite was preserved after the CMS-g-PLA/magnetite formulation (magnetization saturation of magnetite is 62.78 emu/g). In the case of magnetic composite (var. II), the saturation magnetization is only 3.04 emu/g and the remanent magnetization 0.32 emu/g under the same magnetic field applied. Differences for the saturation magnetization of the two types of composites are due fact that in the variant 1, the load theoretical of magnetite was 40 wt.%, while for variant II 4.24 wt.%. Therefore,

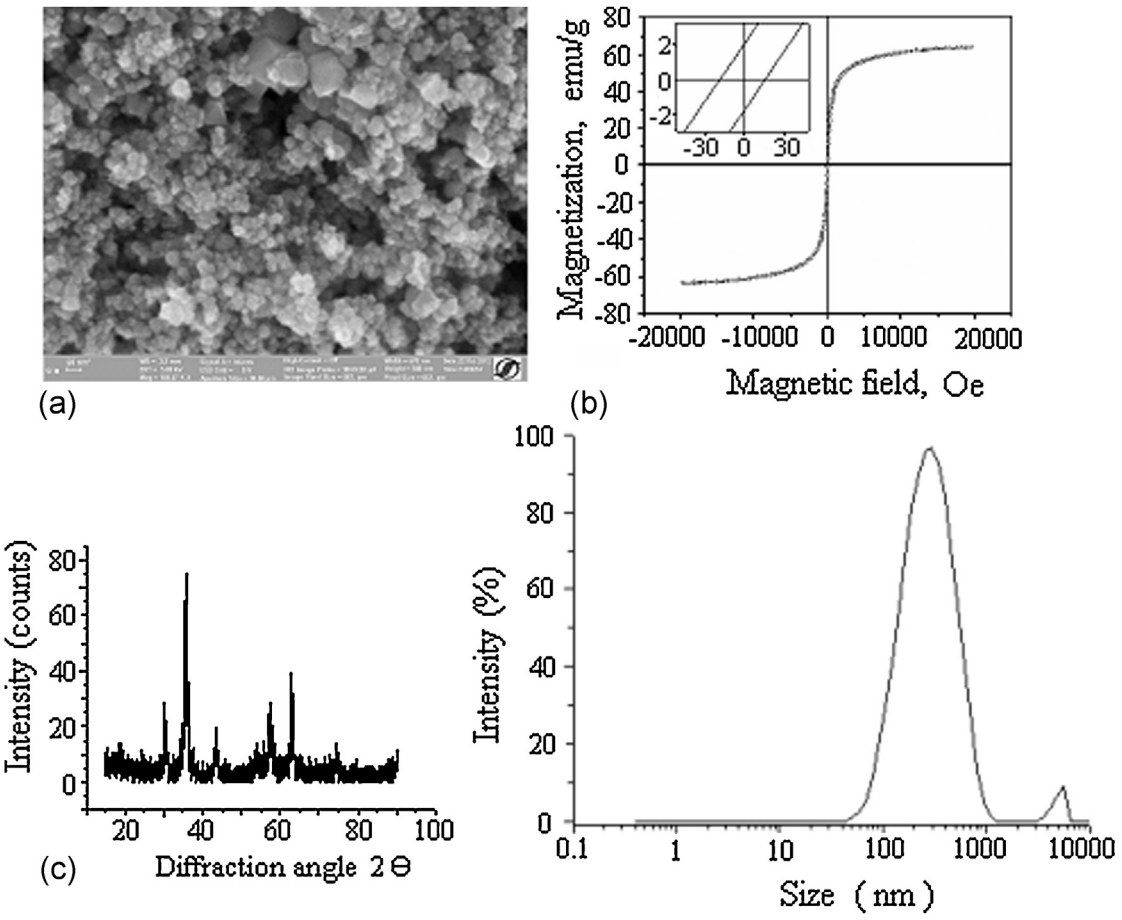

Fig. 3. The magnetic nanoparticles: a – SEM image; b – magnetization; c – X-ray diffraction; d – dimensional distribution of magnetite.

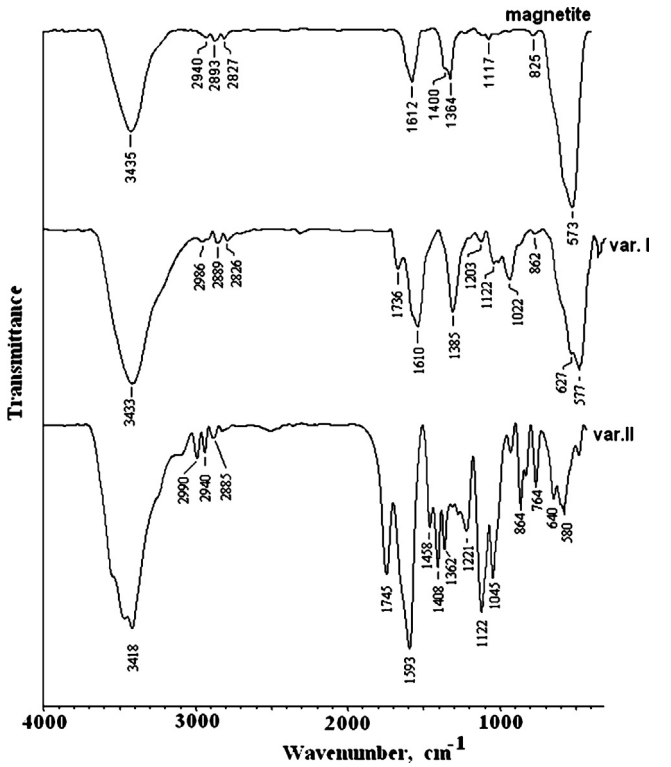

Fig. 4. FTIR spectra of magnetite and of composites prepared through variants I and II.

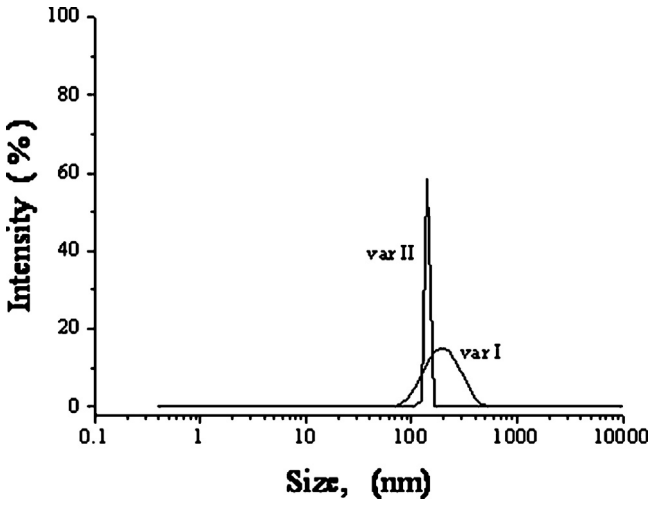

Fig. 5. Size distribution of the CMS-g-PLA/magnetite composites variants I and II.

the found values for the saturation magnetization depend on the magnetite fraction in the magnetic composite.

3.2.4. NIR-CI spectroscopy

The homogeneity of the magnetite distribution in the composites was evaluated with statistical analysis by near infrared chemical imaging spectroscopy. NIR-CI spectroscopy provides information about qualitative and quantitative analysis, and the spatial distribution of the chemical species in the magnetic composites, thus enabling to determine the degree of chemical and/or

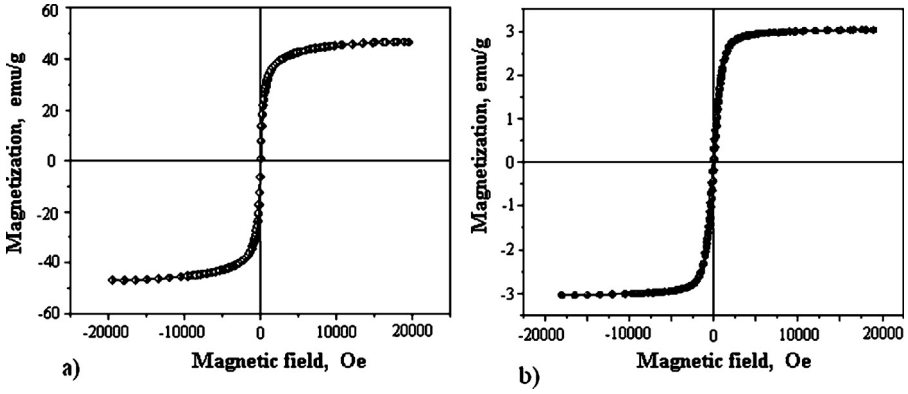

Fig. 6. Magnetization of nanocomposites prepared through variants I (a) and II (b).

physical heterogeneity. The micrographs presented in Fig. 7, shows the score images obtained for CMS-g-PLA matrix, magnetite, and composite. For copolymer and magnetite the white and black colors were attributed, and the gray color corresponds to the magnetic composite. The fact that the black color is predominant in CMS-g-PLA/magnetite (variant I of synthesis) suggests that the magnetite is predominantly and relatively uniform dispersed in the polymer matrix. However, in this variant, magnetite has a tendency of agglomeration, evidenced as well by the particle size. The predicted value of the spatially averaged content of magnetite in the composites is about 57.4 wt.% for the first variant of preparation and about 9.8 wt.% for the second one. The composite with magnetite included *in situ* during preparation shows its uniform and homogeneous distribution and the particle size is much smaller. The predicted values in both cases are higher than those theoretical due to the repeated precipitation and washing operations of the composites, which leads to remove certain percentage of the organic phase. Furthermore, the prediction is influenced by the fact that between structural units of the copolymer and magnetite are some chemical bonds, and NIR spectroscopy is more accurate in the case of physical mixtures.

3.3. Thermogravimetric analyses

The thermogravimetric curves (TG and DTG) of magnetite, CMS-g-PLA copolymer, CMS-g-PLA/magnetite composites are shown in Fig. 8 and thermal parameters are presented in Table 2. The magnetite recorded a weight loss of 6.5 wt.% up to 620 °C, compared with the CMS-g-PLA copolymer whose weight loss reaches up to 72.2 wt.%. Magnetite mass loss of 6.5 wt.% is attributed to Pluronic F127 stabilizer used for nanoparticles preparation. By the addition of magnetite in the polymer matrix (physical by mixing and

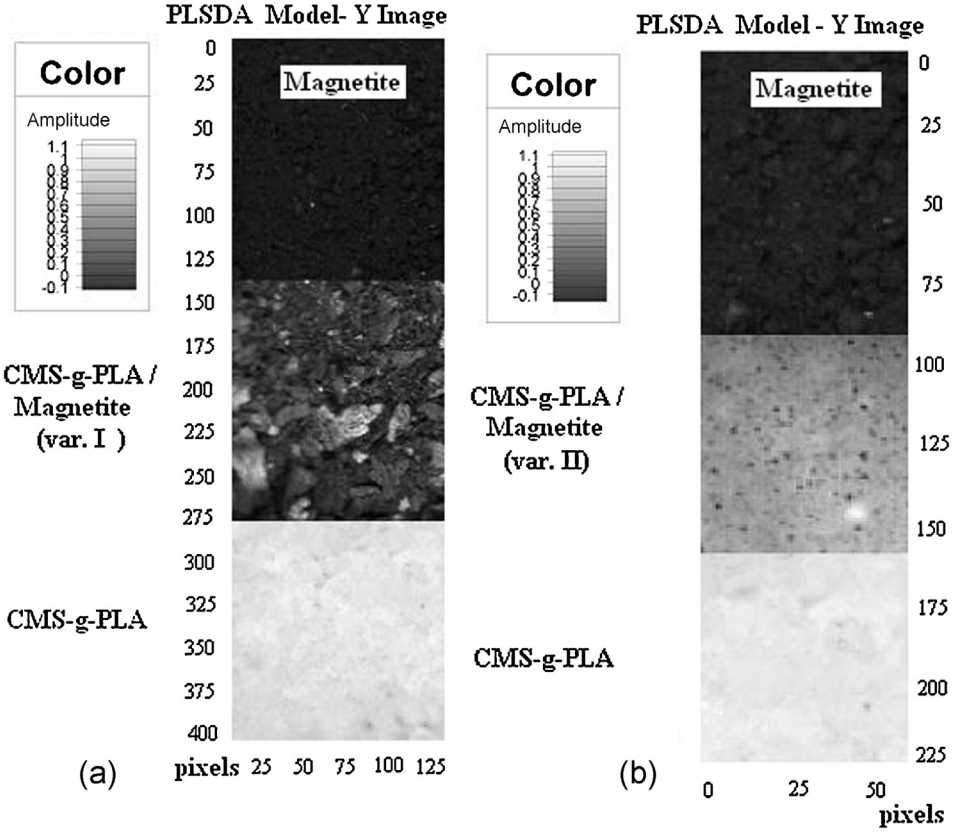

Fig. 7. The score images of CMS-g-PLA/magnetite composites processed accordingly to variant I (a) and II (b) of preparation.

Table 2
Thermogravimetric data.

Sample	Degradation stage	T_{onset} (°C)	T_{peak} (°C)	T_{end} (°C)	W (wt.%)	T_{10} (°C)	T_{50} (°C)
Magnetite	I	128	229	243	2.85		
	II	301	331	359	2.70	–	–
	III	382	415	477	0.93		
	Residue				*93.52*		
CMS-g-PLA	I	87	90	124	6.10		
	II	187	237	260	32.44	179	295
	III	273	289	332	24.92		
	IV	393	419	457	8.74		
	Residue				*27.80*		
CMS-g-PLA/magnetite (variant I)	I	65	79	94	1.00		
	II	128	218	233	7.80		
	III	259	285	329	13.60	250	–
	IV	361	432	445	3.50		
	V	515	554	576	2.90		
	Residue				*71.20*		
CMS-g-PLA/magnetite (variant II)	I	52	83	132	3.75		
	II	165	225	244	13.27	212	342
	III	263	286	313	27.43		
	IV	321	327	351	12.22		
	V	422	459	553	11.16		
	Residue				*32.17*		

Parameters: 10 °C min^{-1}, N_2, Al_2O_3, 30–620 °C; T_{onset} – the temperature at which the thermal decomposition begins; T_{peak} – the temperature at which the degradation rate is maximum; T_{endset} – the temperature at end of the process; T_{10}, T_{50} – the temperature corresponding to 10 and 50 wt.% weight loss; W – weight loss.

precipitating or *in situ*), the composite thermal stability changes depending on the percentage of magnetite used. The percentage of magnetite determined gravimetrically from thermal analyses was calculated considering the residue resulted from thermal decomposition at temperature of 620 °C of magnetic composites and copolymer. Thus, for the magnetic composite variant I was 71.20 – 27.80 = 43.40 wt.%), and for the magnetic composite variant II was 32.17 – 27.80 = 4.37 wt.%).

In the case of magnetic composite *in situ* prepared (variant II), whose content of magnetite added in the synthesis was to 4.24 wt.% (determined by thermogravimetry 4.37 wt.%), the thermal stability increased compared to the stability of PLA-g-CMS copolymer. The weight loss of 10 wt.% (T_{10}) for CMS-g-PLA copolymer has occurred up to 179 °C (Table 1), while in the magnetic composite (variant II) held to 212 °C. In the case of magnetic composite (variant I) the theoretical percentage of magnetite was 40 wt.% (determined by thermogravimetry 43.4 wt.%), and 10 wt.% weight loss occurred up to 250 °C. The differences between the percentages of magnetite determined by thermogravimetry, compared to the theoretical ones are attributed the washing operations of the magnetic composites, which change the polymer/magnetite ratio. At the same time, the mass losses of 50 wt.% (T_{50}) in copolymer took place up to 295 °C, and in the magnetic composite (variant II) to 342 °C, while in the case of composite obtained by dispersion and precipitation the percentage of magnetite was higher and thermal degradation was reduced (residue 71.20 wt.%) and T_{50} parameter could not be determined.

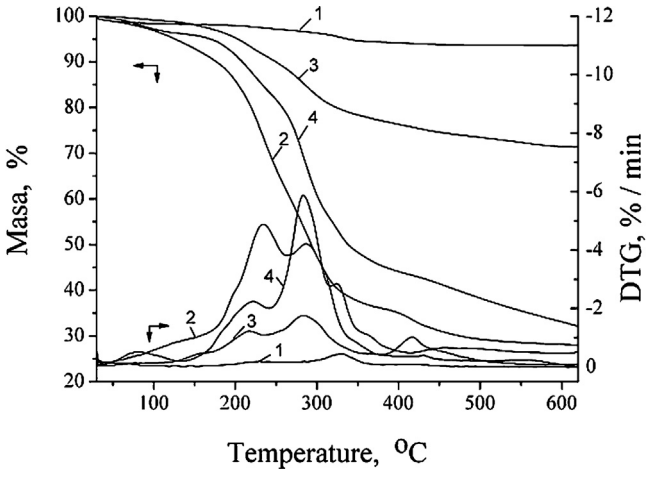

Fig. 8. TG and DTG curves: 1 – magnetite; 2 – CMS-g-PLA copolymer; 3 – CMS-g-PLA/magnetite (variant I); 4 – CMS-g-PLA/magnetite (variant II).

4. Conclusions

The CMS-g-PLA copolymer, synthesized by grafting reaction of carboxymethyl starch with D,L-lactic acid was used to obtain magnetic nanocomposites. The composite materials with magnetic properties were prepared by the precipitation method in acetone of solutions in DMSO of magnetite and copolymer, and *in situ* synthesis. In the first case, the magnetic composite particle size was 168 nm, and the magnetization 46.82 emu/g, while the composite materials showed smaller size (141 nm) for *in situ* synthesis, but with the magnetization more reduced (3.04 emu/g). Higher magnetization in the first case is due to the great degree of encapsulation of the magnetite, which was about 43.4 wt.%, compared to just 4.37 wt.% for *in situ* synthesis (data obtained from thermogravimetry analyses). The copolymers and magnetic nanocomposite structures and the spatial distribution of the components into samples were confirmed by FT-IR and NIR-CI spectroscopy. The FT-IR spectra proved the adsorption of CMS-g-PLA copolymer onto the Fe_3O_4 surface. The CMS-g-PLA-coated magnetic nanoparticles having a core–shell structure with magnetic core and polymeric shell have been successfully prepared. Since CMS-g-PLA is a biodegradable copolymer and the Fe_3O_4 nanoparticles are compatible and tolerated by the human body, these composites can be used for potential applications in the medical field.

Acknowledgments

The authors are grateful for the financial support from the Romanian National Authority for Scientific Research CNCS-UEFISCDI, project: Interdisciplinary research on multifunctional

hybrid particles for bio-requirements "INTERBIORES" PN-II-PT-PCCA-2011-3.2-0428, Grant 211/2012.

References

Al-Deena, F. N., Selomulya, C., & Williams, T. (2013). On designing stable magnetic vectors as carriers for malaria DNA vaccine. *Colloids and Surfaces B: Biointerfaces*, *102*, 492–503.

Anderson, J., & Shive, M. (1997). Biodegradation and biocompatibility of PLA and PLGA microspheres. *Advanced Drug Delivery Reviews*, *28*, 5–24.

Assaad, E., Wang Yu, J., Zhu, X. X., & Mateescu, M. A. (2011). Polyelectrolyte complex of carboxymethyl starch and chitosan as drug carrier for oral administration. *Carbohydrate Polymers*, *84*, 1399–1407.

Baba, D., Seiko, Y., Nakanishi, T., Zhang, H., Arakaki, A., Matsunaga, T., et al. (2012). Effect of magnetite nanoparticles on living rate of MCF-7 human breast cancer cells. *Colloids and Surfaces B: Biointerfaces*, *95*, 254–257.

Barratt, G. M. (2000). Therapeutic applications of colloidal drug carrier. *Pharmaceutical Science and Technology Today*, *3*, 163–171.

Barrat, G., Courraze, G., Couvreur, C., Fattal, E., Gref, R., Labarre, D., et al. (2000). Polymeric micro- and nanoparticles as drug carriers. In S. Dumitriu (Ed.), *Polymeric Biomaterials* (2nd ed., pp. 753–781). New York: Marcel Dekker Inc.

Blanco, M. D., & Alonso, M. J. (1997). Development and characterization of protein-loaded poly(lactide-co-glycolide) nanospheres. *European Journal of Pharmaceutics and Biopharmaceutics*, *43*, 287–294.

Brigger, I., Dubernet, C., & Couvreur, P. (2002). Nanoparticles in cancer therapy and diagnosis. *Advanced Drug Delivery Reviews*, *54*, 631–651.

Bucak, S., Jones, D. A., Laibinis, P. E., & Hatton, T. A. (2003). Protein separations using colloidal magnetic nanoparticles. *Biotechnology Progress*, *19*, 477–484.

Chorny, M., Fishbein, I., Danenberg, H., & Golomb, G. (2002). Lipophilic drug loaded nanospheres prepared by nanoprecipitation: Effect of formulation variables on size, drug recovery and release kinetics. *Journal of Controlled Release*, *83*, 389–400.

Chung, E. Y., Kim, H. M., Lee, G. H., Kwak, B. K., Jung, J. S., Kuh, H. J., et al. (2012). Design of deformable chitosan microspheres loaded with superparamagnetic iron oxide nanoparticles for embolotherapy detectable by magnetic resonance imaging. *Carbohydrate Polymers*, *90*, 1725–1731.

Cornell, R. M., & Schwertmann, U. (1996). *The iron oxide: structure, properties, reactions, occurrence and uses*. Weinheim: VCH.

Fjellvag, H., Gronvold, F., Stolen, S., & Hauback, B. C. (1996). On the crystallographic and magnetic structures of nearly stoichiometric iron monoxide. *Journal of Solid State Chemistry*, *124*, 52–57.

Ghosh, S. (2004). Recent research and development in synthetic polymer-based drug delivery systems. *Journal of Chemical Research*, *4*, 241–246.

Hans, M. L., & Lowman, A. M. (2002). Biodegradable nanoparticles for drug delivery and targeting. *Current Opinion Solid State Matter Science*, *6*, 319–3127.

Hara, K., Tsujimoto, H., Huang, C. C., Kawashima, Y., Mimura, H., & Miwa, N. (2006). The effect of poly(aspartic acid-co-lactic acid) nanospheres on the lung metastasis of B16BL6 melanoma cells by intravenous administration. *Oncology Reports*, *16*, 1215–1220.

Jiang, Q., Gao, W., Li, X., Liu, Z., Huang, L., & Xiao, P. (2011). Synthesis and properties of carboxymethyl *Pueraria thomsonii* Benth. starch. *Starch/Stärke*, *63*, 692–699.

Kouassi, G. K., Irudayaraj, J., & McCarty, G. (2005). Activity of glucose oxidase functionalized onto magnetic nanoparticles. *Biomagnetic Research and Technology*, *3*, 1–10.

Kreuter, J. (1994). Nanoparticles. In J. Kreuter (Ed.), *Colloidal drug delivery systems* (pp. 219–342). New York: Marcel Dekker, Inc.

Lawal, O. S., Lechner, M. D., & Kulicke, W. M. (2008). The synthesis conditions, characterization and thermal degradation studies of an estherified starch from an unconventional source. *Polymer Degradation and Stability*, *93*, 1520–1528.

Lee, S. J., Jeong, J. R., Shin, S. C., Kim, J. C., Chang, Y. H., Chang, Y. M., et al. (2004). Nanoparticles of magnetic ferric oxides encapsulated with poly(D,L lactide-co-glycolide) and their applications to magnetic resonance imaging contrast agent. *Journal of Magnetism and Magnetic Materials*, *272–276*, 2432–2433.

Levy, L., Sahoo, Y., Kim, K. S., Bergey, E. J., & Prasad, P. N. (2002). Nanochemistry: Synthesis and characterization of multifunctional nanoclinics for biological applications. *Chemistry of Materials*, *14*, 3715–3721.

Lu, A. H., Salabas, E. L., & Schuth, F. (2007). Magnetic nanoparticles: Synthesis, protection, functionalization and application. *Angewandte Chemie International Edition*, *46*, 1222–1244.

Ma, M., Zhang, Y., Yu, W., Shen, H. Y., Zhang, H. Q., & Gu, N. (2003). Preparation and characterization of magnetite nanoparticles coated by amino silane. *Colloid and Surfaces A: Physicochemical and Engineering Aspects*, *212*, 219–226.

Ma, Z. Y., Guan, Y. P., & Liu, H. Z. (2005). Synthesis and characterization of micronsized monodisperse superparamagnetic polymer particles with amino groups. *Journal of Polymer Science Part A: Polymer Chemistry*, *43*, 3433–3439.

Nakache, E., Poulain, N., Candau, F., Orecchioni, A. M., & Irache, J. M. (2000). Biopolymer and polymer nanoparticles and their biomedical applications. In H. S. Nalwa (Ed.), *Handbook of nanostructured materials and nanotechnology: organics, polymers, and biological materials* (pp. 577–635). San Diego: Academic Press.

Oster, C. G., Wittmar, M., Unger, F., Barbu-Tudoran, L., Schaper, A. K., & Kissel, T. (2004). Design of amine-modified graft polyesters for effective gene delivery using DNA-loaded nanoparticles. *Pharmaceutical Research*, *21*, 927–931.

Pankhurst, Q., Connolly, J., Jones, S., & Dobson, J. (2003). Applications of magnetic nanoparticles in biomedicine. *Journal of Physics D: Applied Physics*, *36*, R167–R181.

Panyam, J., & Labhasetwar, V. (2003). Biodegradable nanoparticles for drug and gene delivery to cells and tissue. *Advanced Drug Delivery Reviews*, *55*, 329–347.

Rahme, K., Gauffre, F., Marty, J. D., Payre, B., & Mingotaud, C. (2007). A systematic study of the stabilization in water of gold nanoparticles by poly(ethylene oxide)–poly(propylene oxide)–poly(ethylene oxide) triblock copolymers. *The Journal of Physical Chemistry C*, *111*, 7273–7279.

Sekhara Rao, G., Satish Kumar, M., Mathivanan, N., & Bhanoji Rao, M. (2003). Nanosuspensions as the most promising approach in nanoparticulate drug delivery systems. *Pharmazie*, *59*, 5–9.

Song, C. X., Labhasetwar, V., Murphy, H., Qu, X., Humphrey, W. R., Shebuski, R. J., et al. (1997). Formulation and characterization of biodegradable nanoparticles for intravascular local drug delivery. *Journal of Controlled Release*, *43*, 197–212.

Stojanovicĭ, Z., Jeremicĭ, K., Jovanovicĭ, S., & Lechnerb, M. D. (2005). Comparison of some methods for the determination of the degree of substitution of carboxymethyl starch. *Starch/Stärke*, *57*, 79–83.

Stojanovicĭ, Z., Jeremicĭ, K., & Jovanovicĭ, S. (2000). Synthesis of carboxymethyl starch. *Starch/Stärke*, *52*, 413–419.

Sui, Y., Cui, Y., Nie, Y., Xia, G. M., Sun, G. X., & Han, J. T. (2012). Surface modification of magnetite nanoparticles using gluconic acid and their application in immobilized lipase. *Colloids and Surfaces B: Biointerfaces*, *93*, 24–28.

Tartaj, P., Morales, M. P., Veintemillas-Verdaguer, S., Gonzalez-Carreno, T., & Serna, C. J. (2003). The preparation of magnetic nanoparticles for applications in biomedicine. *Journal of Physics D: Applied Physics*, R182–R197.

Tudorachi, N., & Chiriac, A. (2008). Particle size analysis of a silver-based composite for biomedical applications. *Journal of Optoelectronic Advanced Materials*, *10*, 382–388.

Xu, X. Q., Shen, H., Xu, J. R., & Li, X. J. (2004). Aqueous-based magnetite magnetic fluids stabilized by surface small micelles of oleolysarcosine. *Applied Surface Science*, *221*(1–4), 430–436.

Xuan, S., Hao, L., Jiang, W., Gong, X., Hu, Y., & Chen, Z. (2007). Preparation of water-soluble magnetite nanocrystals through hydrothermal approach. *Journal of Magnetism and Magnetic Materials*, *308*(2), 210–213.

Wang, K., Xing, J. F., Li, X. Y., Fu, Q., & Li, W. F. (2012). Fabrication of novel magnetic nanoparticles-coated p(styrene–itaconic acid–divinylbenzene) microspheres. *Carbohydrate Polymers*, *87*, 2712–2717.

Yan, P., Huiying, Z., Hui, X., Gang, W., Jinsong, H., & Junming, Z. (2002). Effect of experimental parameters on the encapsulation of insulin-loaded poly(lactide-co-glycolide) nanoparticles prepared by a double emulsion method. *Journal of Chinese Pharmaceutical Science*, *11*(1), 38–40.